SLAC-PUB-14376

Triple modulator-chicane scheme for seeding sub-nanometer x-ray free electron lasers

Dao Xiang and Gennady Stupakov

SLAC National Accelerator Laboratory, Menlo Park, CA, 94025, USA

(Dated: April 1, 2011)

Abstract

We propose a novel triple modulator-chicane (TMC) scheme to convert external input seed to shorter wavelengths. In the scheme high power seed lasers are used in the first and third modulator while only very low power seed is used in the second modulator. By properly choosing the parameters of the lasers and chicanes, we show that ultrahigh harmonics can be generated in the TMC scheme while simultaneously keeping the energy spread growth much smaller than beam's initial slice energy spread. As an example we show the feasibility of generating significant bunching at 1 nm and below from a low power ($\sim$ 100 kW) high harmonic generation seed at 20 nm assisted by two high power ($\sim$ 100 MW) UV lasers at 200 nm while keeping the energy spread growth within 40%. The supreme up-frequency conversion efficiency of the proposed TMC scheme together with its unique advantage in maintaining beam energy spread opens new opportunities for generating fully coherent x-rays at sub-nanometer wavelength from external seeds.

Work supported in part by US Department of Energy contract DE-AC02-76SF00515.

Free electron lasers (FELs) can provide tunable high-power coherent radiation which has wide applications in biology, chemistry, physics and material science, etc. In x-ray wavelength range, most of the FELs operate in the self-amplified spontaneous emission (SASE) mode [1, 2]. One FEL working in the SASE mode has been successfully operated at hard x-ray wavelengths [3], which marks the beginning of a new era of x-ray sciences [4–6]. While the radiation from a SASE FEL has excellent transverse coherence, it typically has rather limited temporal coherence and relatively large statistical fluctuations because a SASE FEL starts from electron beam shot noise. There are many applications that require, or could benefit from, improved temporal coherence. Seeding the FELs with external coherent laser pulse not only improves the temporal coherence of the radiation, but also provides an FEL signal with well-defined timing with respect to the seed laser, thus allowing pump-probe experiment to be performed with high temporal resolution.

The most direct way to seed an FEL is to use an external coherent source of radiation and the undulator tuned to the same wavelength to amplify the seed. In additional to the requirement on coherence, to achieve a fully coherent FEL output the intensity of the seed should be high enough to dominate over beam shot noise. Seeding at 160 nm from a high harmonic generation (HHG) source has been demonstrated in [7]. Direct seeding with HHG source at 38 nm is under study at FLASH [8] and seeding at $\sim$10 nm is being considered in several FEL projects [9–11]. Seeding with HHG source at even shorter wavelength ($\sim$ 1 nm and below) is believed to be difficult because of the relatively low power of the HHG seed.

To circumvent the need for high power seed at short wavelength, several frequency up-conversion techniques [12–18] have been envisioned to convert the external seed to shorter wavelength. These techniques typically use seeds at UV wavelength where high power lasers are available together with dispersive elements (i.e. chicanes) to generate density modulation at a shorter wavelength in electron beam. The beam is then injected into a long undulator tuned to some harmonic frequency of the seed, and the bunching on that harmonic frequency generates a powerful coherent signal to dominate over beam shot noise so that a fully coherent FEL output is obtained.

Among the several frequency up-conversion schemes, the recently proposed echo-enabled harmonic generation (EEHG) which uses a double modulator-chicane system has the highest up-conversion efficiency [15, 16]. The key advantage of the EEHG scheme is that the

bunching factor of the high harmonics is a slow decaying function of the harmonic number so that relatively small energy modulation can lead to considerable bunching at very high harmonic number. Recent studies showed that EEHG was capable of generating soft x-rays with wavelength of a few nm from UV seed lasers in a single stage [16, 19, 20]. Further extension of the radiation wavelength to 1 nm and below with EEHG is possible, but will most likely involve a large chicane with strong momentum compaction that makes the preservation of the phase space correlations technically challenging. Also the final energy spread will be much larger than the initial value due to the energy modulation in the modulators.

While tremendous progress has been made in seeding the FELs, there is no clear path on how to extend the radiation wavelength to sub-nanometer wavelength. In this paper we propose a triple modulator-chicane (TMC) scheme for seeding sub-nanometer x-ray FELs. We will show that the TMC scheme can make full use of the low power HHG seed such that ultrahigh harmonics can be generated while the energy spread growth is kept much smaller than beam's initial slice energy spread.

The layout of the TMC scheme is schematically shown in Fig. 1. As indicated by the name, the TMC scheme consists of three modulators (M1, M2 and M3) and three chicanes with dispersive strength characterized by factors $R_{56}^{(1)}$, $R_{56}^{(2)}$ and $R_{56}^{(3)}$, respectively. Here we will limit ourselves to the scenario when the lasers in M1 and M3 have the same wavelength, but π phase difference, and the first and the second chicanes have the opposite momentum compaction factors ($R_{56}^{(2)} = -R_{56}^{(1)}$).

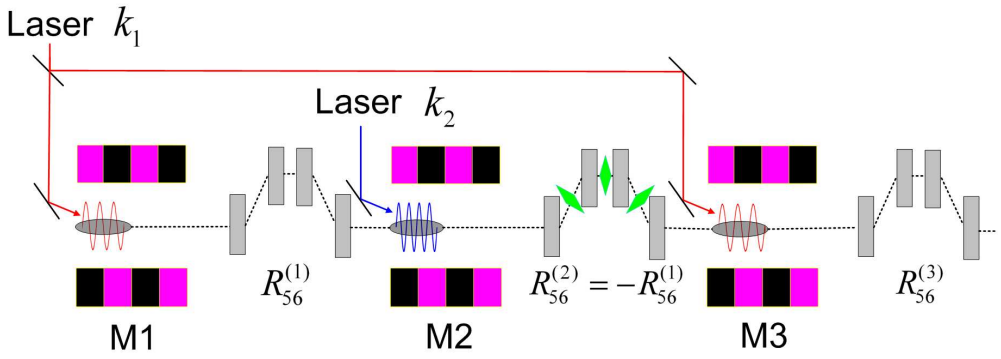

FIG. 1: Schematic of the triple modulator-chicane scheme. A laser with wave number k_1 is used in M1 and M3. Another laser with wave number k_2 is used in M2. The first and third chicanes are simple 4-bend chicanes while the second chicane has some quadrupoles (shown by green diamonds) in it to provide a momentum compaction with opposite sign.

Following the analysis in [15, 16], we assume the bunch length is much larger than the wavelength of the lasers so that we can assume a longitudinally uniform beam of which the initial longitudinal phase space distribution is $f_0(p) = N_0(2\pi)^{-1/2}e^{-p^2/2}$, where N_0 is the number of electrons per unit length of the beam, $p = (E - E_0)/\sigma_E$ is the dimensionless energy deviation of a particle, E_0 is the average beam energy and σ_E is the rms energy spread. After interaction with the laser with wave number k_1 in M1, particle's energy changes to $p' = p + A_1 \sin(k_1 z)$, where $A_1 = \Delta E_1/\sigma_E$, ΔE_1 is the energy modulation amplitude and z is the longitudinal coordinate in the beam. The distribution function after the interaction with the laser becomes $f_1(\zeta, p) = N_0(2\pi)^{-1/2} \exp\left[-(p - A_1 \sin\zeta)^2/2\right]$, where $\zeta = k_1 z$. Sending the beam through the first chicane converts the longitudinal coordinate z into z', $z' = z + R_{56}^{(1)} p\, \sigma_E/E_0$, and makes the distribution function $f_2(\zeta, p) = N_0(2\pi)^{-1/2} \exp\left[-\left(p - A_1 \sin(\zeta - B_1 p)\right)^2/2\right]$, where $B_1 = R_{56}^{(1)} k_1 \sigma_E/E_0$. Note for the chosen coordinates with bunch head at $z > 0$, the momentum compaction of a simple 4-bend chicane is positive. Negative momentum compaction can be obtained by adding quadrupoles in the 4-bend chicane.

The final distribution function at the exit from the third chicane can be easily found by applying consecutively four more transformations to $f_2(\zeta, p)$. The first and third of these four transformations corresponding to the modulation in M2 and M3. The second and fourth one corresponding to the passage through the second and the third chicane. The final distribution function under the condition $R_{56}^{(2)} = -R_{56}^{(1)}$, $k_3 = k_1$ and $\phi_2 = \pi$ is:

$$\begin{aligned} f_f(\zeta, p) = N_0(\sqrt{2\pi})^{-1} \exp\Big[& -(1/2)\big[p + A_3 \sin(\zeta - B_3 p) \\ & - A_2 \sin[K(\zeta - B_3 p) + K B_1 (p + A_3 \sin(\zeta - B_3 p)) \\ & + \phi_1] - A_1 \sin[(\zeta - B_3 p) + A_2 B_1 \sin[K(\zeta - B_3 p) \\ & + K B_1 (p + A_3 \sin(\zeta - B_3 p)) + \phi_1]]\big]^2 \Big], \end{aligned} \tag{1}$$

where $A_{2,3}$, $k_{2,3}$ and $\phi_{1,2}$ are the dimensionless energy modulation, the wave number and phase of the laser in M2 and M3, $B_3 = R_{56}^{(3)} k_1 \sigma_E/E_0$, and $K = k_2/k_1$.

Integration of Eq. (1) over p gives the beam density N as a function of ζ, $N(\zeta) = \int_{-\infty}^{\infty} dp f_f(\zeta, p)$. We define the bunching factor b as $b = \frac{1}{N_0}|\langle e^{-ia\zeta} N(\zeta)\rangle|$, where a is a number, and the brackets denote averaging over the coordinate ζ. Analysis shows the bunching factor is not zero only if $a = n + Km$ which means presence of a modulation with the wave number $k_T \equiv a k_1 = n k_1 + m k_2$, where n and m are integer numbers. After some mathematical

manipulation, we found the bunching factor is,

$$
\begin{aligned}
b_{n,m} = & \sum_{j=-\infty}^{\infty} e^{-\frac{1}{2}(B_3(Km+n)-B_1Km)^2+im\phi_1)} \\
& \times J_m\left(A_2B_1j + A_2\left(B_1 - B_3\right)\left(Km+n\right)\right) \\
& \times J_j\left(-A_3B_3(Km+n)\right) \\
& \times J_{n+j}\left(A_1B_1Km - A_1B_3(Km+n)\right) . \qquad (2)
\end{aligned}
$$

For given harmonic number a and energy modulation A_1, analysis shows that minimal energy spread growth is achieved when $A_3 = A_1$, and in this case optimal bunching is achieved when $B_1 \approx a/A_1K$, $A_2 \approx A_1K/a$ and $B_3 \approx 1/A_1$.

To illustrate the physics behind the TMC scheme, the evolution of the beam longitudinal phase space is shown in Fig. 2. For simplicity, we assume the lasers have the same wavelength in the three modulators and only the phase space within one wavelength region is shown. The parameters used to obtain Fig. 2 are as follows: $A_1 = A_3 = 5$, $A_2 = 0.05$, $B_1 = -B_2 = 4.7$ and $B_3 = 0.176$.

The beam phase space after interaction with the first laser is shown in Fig. 2a. The modulation introduces a local energy chirp, defined as $h = dp/d\zeta$, into beam's longitudinal phase space. Similar to the EEHG scheme, separated energy bands are generated (Fig. 2b) after beam passing through the first chicane which has a large momentum compaction ($B_1 = 4.7$). For the particles around the zero-crossing of the laser ($h_1 = A_1$), the compression factor in the first chicane is $C_1 = 1/(1 + h_1B_1) \approx 1/A_1B_1$. Because of the large B_1, the modulation is locally decompressed in the first chicane, which leads to separated energy bands in beam phase space with a spacing of about $2\pi\sigma_E/B_1$ and the rms energy spread for each band roughly equals to $C_1\sigma_E \approx \sigma_E/A_1B_1$. Accordingly, the chirp is reduced to $h_2 = C_1h_1 \approx 1/B_1$.

After interaction with the second laser with $A_2 = 0.05$, the beam phase space evolves to that in Fig. 2c. Because the energy modulation is much smaller than beam's initial energy spread, it is actually very difficult to see the difference in Fig. 2b and Fig. 2c. The second chicane with $B_2 = -4.7$ compresses the beamlets with a compression factor $C_2 \approx A_1B_1$ and amplifies the modulation imprinted in M2. The resulting beam phase space is shown in Fig. 2d which is similar to that in Fig. 2a. If $A_2 = 0$, the second chicane should restore the beam phase space to the same distribution as that before the first chicane. As long as C_2A_2

is not much larger than unity, the second chicane will transform the beam phase space to a distribution similar to that before the first chicane with the presence of energy modulation from M2 superimposed on the modulation from M1 (Fig. 2d).

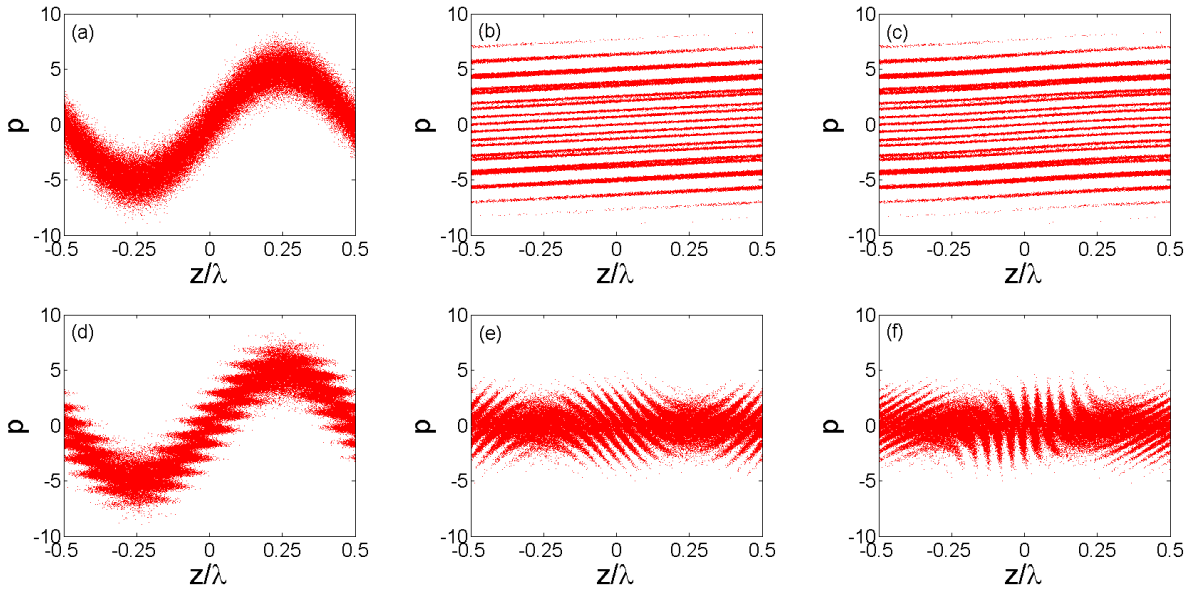

FIG. 2: Longitudinal phase space evolution in TMC scheme: (a)-After the first modulator; (b)-After the first chicane; (c)-After the second modulator; (d)-After the second chicane; (e)-After the third modulator; (f)-After the third chicane.

The laser in M3 is chosen to give the beam the same modulation amplitude ($A_3 = 5$) as that in M1, but with a π phase shift, so that the overall energy modulation in M1 is canceled in M3. After the cancelation, the modulation from M2 becomes dominant, as shown in Fig. 2e. The wavelength of the modulation in Fig. 2e is roughly C_2 times smaller than that in M2. A third chicane with small momentum compaction ($B_3 = 0.176$) further converts the energy modulation into density modulation (Fig. 2f). Using the particle distribution in Fig. 2f, we found that significant bunching (7%) at the harmonics around $a = 22$ is generated with a modulation in M2 that is 20 times smaller than beam slice energy spread.

Due to the effective cancelation of the energy modulation in M1 and M3, the final energy spread growth (about 15%) is mainly from the modulation in M2. Since in the TMC scheme only a very small energy modulation (typically comparable to the energy spread of each energy band) is needed in M2, the final energy spread growth can be controlled to a very low level.

The unique advantages of TMC scheme that only a small energy modulation is needed in M2 and the second chicane compresses the modulation imprinted in M2 to shorter wavelength opens new opportunities for using HHG source to seed x-ray FELs. Here we show how one can generate bunching at 1 nm and below using TMC scheme with the low power HHG source as the seed in M2. As an example, we assume the HHG source has a wavelength of 20 nm and the wavelength of the lasers in M1 and M3 are 200 nm. The electron beam parameters used in following analysis are similar to those in the proposed high rep-rate FEL at LBNL [19] with beam energy $E = 2.4$ GeV and slice energy spread $\sigma_E = 150$ keV.

For $A_1 = A_3 = 3$, $A_2 = 0.1$, $B_1 = -B_2 = 6.46$ and $B_3 = 0.327$, the longitudinal phase space at the exit of the third chicane simulated with our 1-D code is shown in Fig. 3a. The total energy spread growth is about 40%. The bunching factor calculated using the particle distribution in Fig. 3a is show in Fig. 3b where one can see that the bunching factor at 1 nm ($a = 200$) is about 5% and there is also considerable bunching (1.5%) at 0.5 nm ($a = 400$). The bunching factor may be large enough to dominate over shot noise and sending the beam through a radiator tuned to the harmonic radiation wavelength may allow generation of fully coherent x-rays at 1 nm.

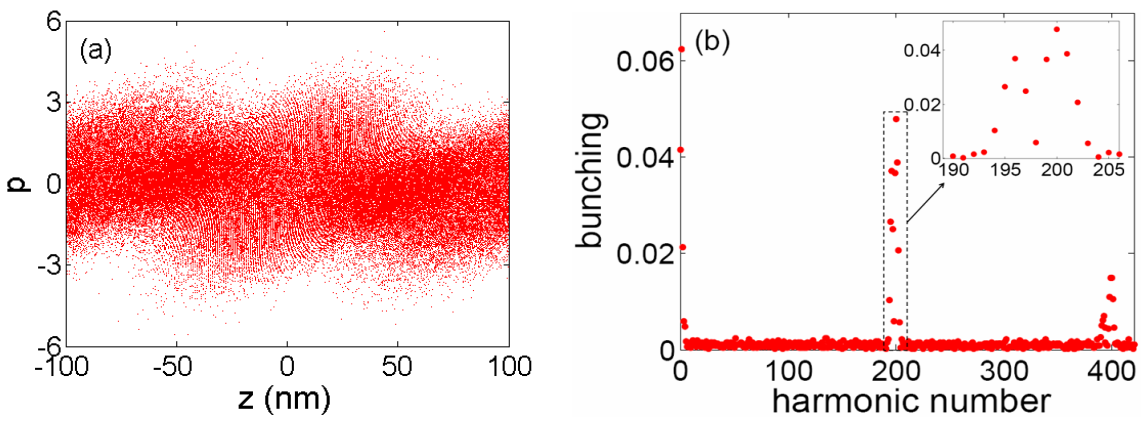

FIG. 3: Beam longitudinal phase space at the exit of the third chicane (a) and the corresponding bunching factor for various harmonic numbers (b).

The required energy modulation (450 keV) in M1 and M3 can be achieved with 100 MW 200 nm lasers with a waist of 0.6 mm (assuming a 10-period modulator with a period length of 15 cm), as estimated with Eq. (14) in [16]. The small energy modulation in M2 (15 keV) can be achieved with a 100 kW HHG source at 20 nm with a waist of 0.4 mm (assuming a

35-period modulator with a period length of 6 cm), which is readily reachable with existing technologies [21]. The required momentum compaction of the first chicane is reasonably small, i.e. $R_{56}^{(1)} = 3.29$ mm. For such a small chicane, analysis shows that the energy spread growth from incoherent synchrotron radiation can be easily controlled to be much smaller than the spacing of the adjacent energy bands so that the phase space correlation can be preserved.

In the analysis above, we assumed that the energy modulation in M1 and M3 are exactly the same and the laser phase difference in M1 and M3 is exactly π. In reality these values may fluctuate. To identify the sensitivity of the performance of the TMC scheme on these fluctuations, we simulated the bunching factor at 1 nm with four sets of two parameters (A_1 and A_3, A_2 and A_3, B_1 and B_3, ϕ_1 and ϕ_2) varied while keeping other parameters at the optimal values (Fig. 4).

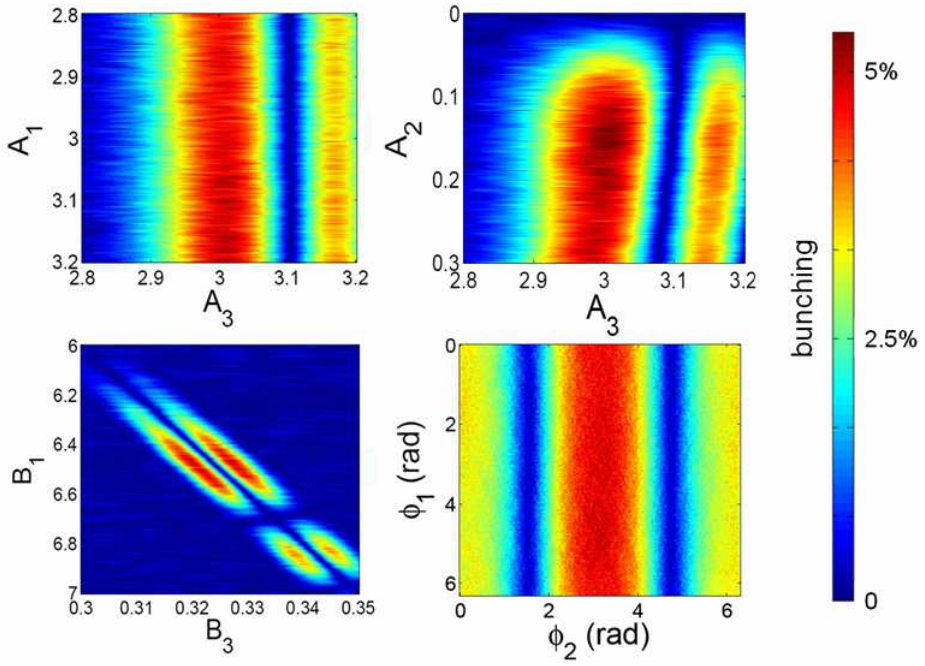

FIG. 4: Bunching factor at 1 nm for various A_1 and A_3 (top left); A_2 and A_3 (top right); B_1 and B_3 (bottom left); ϕ_1 and ϕ_2 (bottom right).

The top-left plot in Fig. 4 shows that the bunching is more sensitive to A_3 than A_1. To maintain a large bunching factor at 1 nm, the power fluctuation of the laser in M3 should be controlled within 4%. While the modulation in M1 only weakly affects the bunching, effective cancelation of energy modulation in M3 still requires its power to be close to that

in M3.

The top-right plot in Fig. 4 indicates that the bunching is not sensitive to the energy modulation in M2, as long as the modulation is not too small. This loosens the requirement on the stability of the HHG seed. Since the bunching frequency is roughly $k_2 B_1/B_3$, the chicane strength needs to controlled within a few percent to provide a large bunching at some given frequency, as can be seen in the bottom-left plot of Fig. 4.

Finally the bottom-right plot shows that the bunching is not sensitive to the phase difference between the first laser and the HHG seed (ϕ_1), but is sensitive to that between the first and third laser (ϕ_2). Large bunching is achieved when ϕ_2 deviates from π within $\pi/4$. From a practical point of view, the lasers in M1 and M3 should originate from the same source so that their relative phase can be accurately controlled by controlling the path length of the lasers. Also the total momentum compaction of the beam line between M1 and M3 should be zero ($B_2 = -B_1$) to maintain a constant time-of-flight of the electron beam, so that the phase difference in the modulations is solely determined by the laser phase difference. It is worth mentioning that if no efforts are made to control the laser phase difference, there is still a probability of 25% to get considerable bunching.

It should be pointed out that the above example is just representative. Bunching the beam at higher harmonics with $a > 200$ can be achieved by either increasing the compression factor ($A_1 B_1$) in the second chicane, or reducing the wavelength of the HHG seed in M2. Note HHG at 4.37 nm with energy > 10 nJ has been obtained [22], and using a HHG seed at 4 nm in the above example may lead to considerable bunching at 2 Ångström.

In summary, we have proposed a new working scheme of harmonic generation in FELs. Compared to other harmonic generation schemes, the TMC scheme has unique advantages that only very low power HHG seed and relatively small chicane is needed, and the total energy spread growth can be controlled to a very low level. It offers a promising solution to achieve fully coherent x-rays in the sub-nanometer wavelength from external seeds. Similar to EEHG, the success of TMC scheme relies on preservation of the long-term memory of beam phase space correlations. While recent EEHG experimental results [23] are encouraging, more theoretical and experiment work is needed in order to fully address the practicality of implementing the TMC scheme at nm and Ångström wavelength. This work was supported

by the US DOE under Contract No. DE-AC02-76SF00515.

---

[1] A. Kondratenko and E. Saldin, Part. Accel. 10, 207 (1980).

[2] R. Bonifacio, C. Pellegrini, and L.M. Narducci, Opt. Commun. 50, 373 (1984).

[3] P. Emma, *et al.*, Nat. Photon. 4, 641 (2010).

[4] L. Young *et al.*, Nature, 466, 56 (2010).

[5] H. Chapman *et al.*, Nature, 470, 73 (2011).

[6] M. Marvin Seibert *et al.*, Nature, 470, 78 (2011).

[7] G. Lambert *et al.*, Nature Phys. 4, 296 (2008).

[8] J. Bödewadt *et al.*, in *Proceedings of FEL 10* (Malmö, Sweden, 2010).

[9] M.E. Couprie *et al.*, in *Proceedings of FEL 08* (Gyeongju, Korea, 2008), p.131.

[10] N.R. Thompson *et al.*, in *Proceedings of FEL 09* (Liverpool, UK, 2009), p.694.

[11] S. Reiche *et al.*, in *Proceedings of FEL 09* (Liverpool, UK, 2009), p.51.

[12] L.-H. Yu, Phys. Rev. A, 44, 5178 (1991).

[13] B.W.J. McNeil, G.R.M. Robb and M.W. Poole, in *Proceedings of 2005 Particle Accelerator Conference* (Knoxville, Tennessee, 2005), p.1718.

[14] E. Allaria and G. De Ninno, Phys. Rev. Lett, 99, 014801 (2007).

[15] G. Stupakov, Phys. Rev. Lett, 102, 074801 (2009).

[16] D. Xiang and G. Stupakov, Phys. Rev. ST-AB, 12, 030702 (2009).

[17] D. Ratner, Z. Huang and A. Chao, Phys. Rev. ST-AB, 14, 020701 (2011).

[18] J. Qiang, Nucl. Instrum. Methods Phys. Res., Sect. A 621, 39 (2010).

[19] D. Xiang and G. Stupakov, in *Proceedings of PAC 09* (IEEE, Vancouver, 2009).

[20] E. Allaria, G. De Ninno and D. Xiang, in *Proceedings of FEL 09* (Liverpool, 2009), p.39.

[21] I Jong Kim *et al.*, Appl. Phys. Lett, 92, 021125 (2008).

[22] M. Zepf *et al.*, Phys. Rev. Lett, 99, 143901 (2007).

[23] D. Xiang *et al.*, Phys. Rev. Lett, 105, 114801 (2010).